HIGH POWER LASER
SCIENCE AND ENGINEERING

RESEARCH ARTICLE

Brightness enhancement on a narrow-linewidth fiber Bragg grating-based master oscillator power amplification fiber laser

Xin Tian[1,2,3,†], Binyu Rao[1,2,3,†], Meng Wang [1,2,3], Xiaoming Xi [1,2,3], Zhixian Li[1,2,3], Zilun Chen[1,2,3], Hu Xiao[1,2,3], Pengfei Ma [1,2,3], and Zefeng Wang [1,2,3]

[1] *College of Advanced Interdisciplinary Studies, National University of Defense Technology, Changsha, China*

[2] *Nanhu Laser Laboratory, National University of Defense Technology, Changsha, China*

[3] *Hunan Provincial Key Laboratory of High Energy Laser Technology, National University of Defense Technology, Changsha, China*

(Received 10 January 2024; revised 11 April 2024; accepted 17 April 2024)

Abstract

In this paper, we have experimentally demonstrated a high-power and high-brightness narrow-linewidth fiber amplifier seeded by an optimized fiber oscillator. In order to improve the temporal stability, the fiber oscillator consists of a composite fiber Bragg grating-based cavity with an external feedback structure. By optimizing the forward and backward pumping ratio, the nonlinear effects and stimulated Raman scattering-induced mode distortion of the fiber amplifier are suppressed comprehensively, accompanied with the simultaneous improvement of beam quality and output power. The laser brightness is enhanced further by raising the threshold of transverse mode instability by approximately 1.0 kW by coiling the gain fiber with a novel curvature shape. Finally, a 6 kW narrow-linewidth laser is achieved with beam quality (M^2) of approximately 1.4. The laser brightness doubled compared to the results before optimization. To the best of our knowledge, it is the highest brightness narrow-linewidth fiber laser based on a one-stage master oscillator power amplification structure.

Keywords: brightness; fiber laser; narrow linewidth; ytterbium-doped fiber

1. Introduction

In recent years, fiber lasers have developed in the direction of higher power, higher brightness and wider applications owing to their compact structure, high conversion efficiency, excellent beam quality and convenient thermal management[1–3]. From the perspective of power scaling of fiber lasers, the pursuit of even higher power is never satisfied. However, the ultimate output power is challenged by transverse mode instability (TMI) and fiber nonlinearities resulting from the increase of density within the fiber core and the long interaction length[4–7]. Besides, the beam quality has to be sacrificed with a larger fiber core for higher power and weaker nonlinear effects. The emergence of both spectral beam combination (SBC) and coherent beam combination (CBC) provides promising methods to break through the limitations of fiber lasers while maintaining good beam quality[8–11]. The power scaling ability of combination systems is dependent on the input power and the number of sub beams combined. Laser brightness, which can be defined as $\beta \propto P/{(M^2)}^2$, is an extremely important parameter for the application of SBC and CBC, where P is the output power and M^2 is the beam quality factor[3]. Thus, developing a high-brightness narrow-linewidth fiber amplifier (NLFA) is critical and highly desired for beam combination technology.

The master oscillator power amplification (MOPA) structure is typically used to realize NLFAs. These fiber amplifiers mainly adopt two types of seed: the phase-modulated single-frequency laser and the fiber oscillator laser. The high-power fiber laser with linewidth less than 10 GHz is useful for CBC, which can be achieved by the MOPA structure seeded by a phase-modulated single-frequency laser and has reached the 2 kW level currently[12–14]. It is usually limited by the stimulated Brillouin scattering (SBS) effect during power scaling due to the ultra-narrow linewidth[15,16]. The higher

Correspondence to: X. Xi and Z. Wang, College of Advanced Interdisciplinary Studies, National University of Defense Technology, Changsha 410073, China. Emails: exixiaoming@163.com (X. Xi); zefeng-wang_nudt@163.com (Z. Wang)

†These authors contributed equally to this paper.

power laser with linewidth less than 1 nm has also been intensively researched, which is useful for the SBC system whose linewidth requirements are not as strict as those of the CBC system. The power scaling of such high-power NLFAs is affected by TMI and various nonlinear effects, including SBS, stimulated Raman scattering (SRS) and four-wave mixing (FWM)[17–23]. In 2022, Ma *et al.*[19] reported a 7.03 kW near-single-mode NLFA with 3 dB linewidth of 0.76 nm, which is based on the phase-modulated single-frequency laser seed. However, the recorded output power of the high-brightness NLFA based on a fiber oscillator laser seed is no more than the 5 kW level[20–23]. The highest reported power is 4.6 kW with 3 dB linewidth of 0.35 nm and M^2 factor of 1.31[23]. The phase-modulated single-frequency laser seed maintains the good properties of the single frequency but has to use a complex multi-stage amplification configuration. The fiber oscillator laser seed has the advantages of a simple one-stage structure, good robustness and low cost, but needs to overcome the nonlinear effects induced by temporal instability. With optimizing the time domain features of the seed and suppressing the nonlinear effects and TMI comprehensively, a NLFA seeded by a fiber oscillator is a potential method with good cost performance.

In this paper, we demonstrate a bi-directional pumping NLFA seeded by a fiber oscillator. The fiber oscillator is based on a composite cavity with an external feedback structure for good temporal stability. By optimizing the bi-directional pumping ratio, the various nonlinear effects are suppressed comprehensively, and the output power and beam quality are improved. Furthermore, the TMI threshold is also improved by approximately 1.0 kW by coiling the gain fiber with a novel curvature shape. Finally, a 6 kW narrow-linewidth output is achieved with an optical-to-optical efficiency of 85.0%. The 3 and 20 dB linewidths are 0.63 and 2.81 nm, respectively. The beam quality is measured to be $M^2 \sim 1.4$ and the signal to Raman ratio is more than 30 dB at the maximum output power. The laser brightness doubled compared to the results before optimization. To the best of our knowledge, this is the reported output power record based on this narrow-linewidth one-stage MOPA fiber laser.

2. Optimization for the seed structure

It has been reported that many strategies, such as a large core, short length gain fiber, a backward pumping structure and a wavelength stabilized laser diode (WS LD), can be used to decrease the linewidth of fiber oscillators[22]. However, even if these methods are employed, self-pulsing and poor temporal characteristics are inevitable when running into narrow-linewidth fiber oscillators. The narrower the bandwidth of the fiber Bragg grating (FBG), the greater the temporal fluctuations of the fiber oscillator laser. Moreover, a seed laser with high peak power self-pulses would lead to a much lower SRS threshold during power

amplification[4,24,25]. Thus, enhancing the temporal stability of the seed is the key for high-power NLFA systems.

Some methods have been studied for improving the temporal characteristics of the fiber oscillator, such as either a composite cavity or external feedback[26–30]. Here, we proposed a novel hybrid structure to combine these two methods, whose schematic diagram is depicted in Figure 1. Different from the conventional Fabry-Perot structure, the fiber oscillator can be treated as a composite cavity with external feedback. A composite cavity utilizing an additional low-reflectivity (LR) FBG with wide bandwidth (WB) outside the oscillator cavity has been reported to improve the temporal stability of the fiber oscillator laser[26]. However, an additional WB-LR FBG contains more longitudinal modes in itself and thus it is not suitable for our narrow-linewidth laser system. Besides, using an additional narrow bandwidth (NB) LR FBG to form a composite cavity is also inappropriate because a slight mismatch of the center wavelength between the two NB-LR FBGs would result in the failure of this strategy, especially when they experience different thermal loads. Therefore, a modified composite cavity with an additional high-reflectively (HR) FBG rather than an LR FBG is adopted in this paper. For the theoretical analysis, one can refer to Ref. [27]. The longitudinal modes of a composite cavity are the combined longitudinal modes with different frequency components from the separate cavity. Simulation results show that the peak and valley points in the temporal intensity of the two frequency components could cancel each other out. Therefore, the temporal fluctuations of the combined two frequency components are less than that of a separate frequency component. Besides, the composite cavity could help select the longitudinal modes with the same frequency so that it reduces the crosstalk between longitudinal modes. In this way, the temporal fluctuations of the seed could be reduced.

Besides, it has been reported that the peak intensity of self-pulses can be weakened and temporal properties can be enhanced after the laser transmits over long passive fibers[28]. However, the signal light injecting amplifier directly would bring about a decrease of the SRS threshold and spectral broadening in the fiber laser system. Here, the long passive fiber is introduced neither in the cavity nor between the seed and the amplifier. As shown in Figure 1, the novel structure utilizes an optical coupler with one arm of the coupler to connect the long passive fiber and the other arm to connect to the amplifier. It is worth noting that the output fiber is not cleaved to 8° but rather at a flat angle (0°), which means that there is approximately 4% signal light at the fiber end reflected into the modified composite cavity. The introduced weak light is generated from the Fresnel reflection and forms the external feedback of the fixed cavity. The feedback light with stable temporal features would affect the temporal features of the longitudinal modes in the cavity, which is different from a random fiber laser
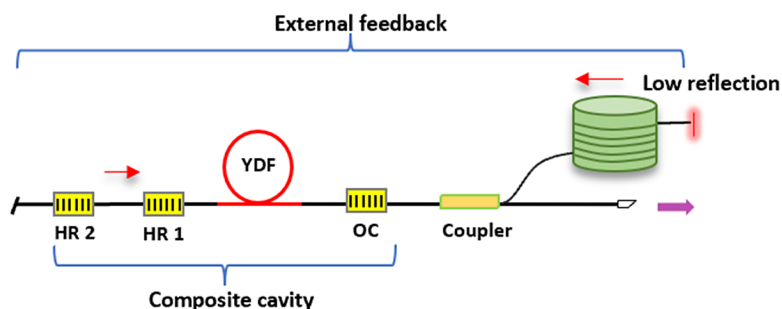
Figure 1. Schematic of the novel cavity.

(RFL) with a modeless spectrum[29]. The use of long fiber feedback in the MOPA system helps to reduce the pulse intensity by nonlinear effects. When the signal laser is transmitting over the long passive fibers, the high-intensity self-pulses would be split into low-intensity pulses due to the self-phase modulation (SPM) effect[30]. Then, the average pulse intensity and temporal fluctuations of the signal could decrease simultaneously. Moreover, the feedback from the Fresnel reflection can be also treated as a composite cavity possessing an additional LR FBG with super WB, which is also helpful to seed stability[26,31]. The effect can be superimposed on long fiber feedback. Essentially, the two methods both break the original coherence characteristics between the effective longitudinal modes and reduce the intensity and gradient distribution of the self-pulses. The temporal features of the seed structure could be enhanced reasonably.

Although the temporal characteristics could be optimized, the influence of the seed structure on the linewidth needs to be taken into account. Because the feedback light from the Fresnel reflection transmits through long passive fiber, the spectrum of the seed laser has the features of feedback light. The 3 dB linewidth of the output laser between the optimized cavity and the traditional cavity without long fiber feedback is almost identical for the limitation of the NB FBG, but the bottom of the signal spectrum is broadened. More importantly, the rate of spectral broadening is different when the two types of signal laser are amplified respectively.

The optimized seed possesses good temporal features so that the spectral broadening effect is weak and the spectral shape can be maintained well, avoiding spectral bottom broadening being severe at high power level[29].

3. Experimental setup

Figure 2 demonstrates the experimental structure based on the optimized seed. A WS LD with center wavelength of 976 nm is used as the pump source of the seed. The HR-FBG 1 and HR-FBG 2 provide reflectivity of approximately 99.5% and 50%, respectively, with the same full width at half maximum (FWHM) of approximately 3 nm. The adopted gain fiber is a double-clad ytterbium-doped fiber (YDF), which has a size of 20/400 μm and a length of approximately 6 m. The absorption coefficient is approximately 0.55 dB/m at 915 nm. The output coupler (OC) FBG has a reflectivity of approximately 10% and an FWHM of approximately 0.05 nm. The pump light is backward injected via a side pump and a signal combiner (SPSC). The residual pump light is removed by a cladding light stripper (CLS 1). The seed power could provide signal power of about 45 W. After the CLS, a 50:50 optical coupler is located after the composite cavity. Half of the power is injected into a long passive fiber with length of approximately 200 m. The end of the passive fiber is cleaved to a flat angle, and thus a Frensel feedback light is reflected into the modified cavity. The other
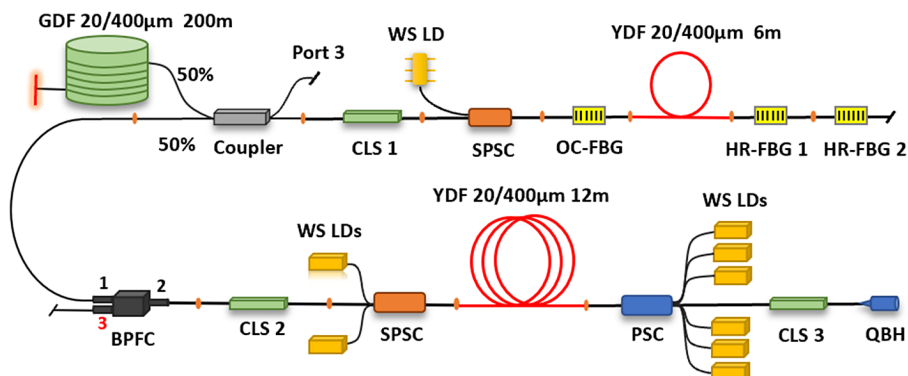

Figure 2. Schematic of the narrow-linewidth MOPA fiber amplifier with a bi-directional pump structure.
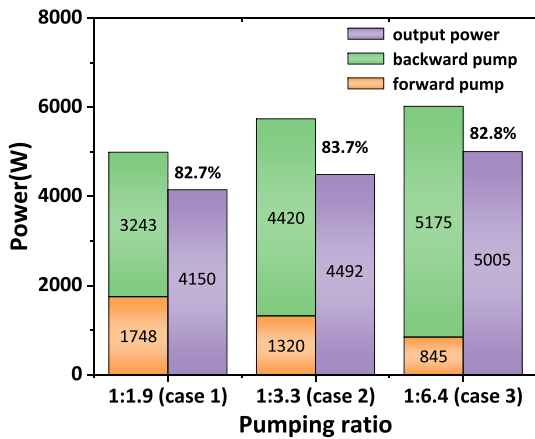
Figure 3. The input and output powers and their conversion efficiency at different pumping ratios.

output arm of the coupler is connected to the main amplifier through a band pass filter circulator (BPFC). Apart from filtering the spectral noise of the injected laser, the BPFC also performs as an SBS monitor by measuring the backward power at port 3. Another CLS is attached after the BPFC in order to remove the residual pump power of the amplifier.

The amplification stage adopts a bi-directional pump structure. The pump source employs eight groups of 976 nm WS LDs with the maximum pump power of approximately 1100 W for each. The forward and backward pump powers were injected via a $(2 + 1) \times 1$ SPSC and a $(6 + 1) \times 1$ pump and signal combiner (PSC), respectively. The SPSCs used in the laser system can effectively maintain the beam quality. The signal fiber sizes of the SPSC and gain fiber are both 20/400 μm. The length of the YDF in the amplifier is approximately 12 m, while the core diameter of the signal fiber of the PSC increases from 20 to 25 μm. Notably, the absorption coefficient of the YDF in the amplification stage is approximately 0.37 dB/m at a wavelength of 915 nm, which is different from that used in the seed. The lower absorption coefficient of the gain fiber is for convenient thermal management and a higher TMI threshold. A CLS and a quartz block head (QBH) are attached for the output. The laser performance, including the output power, optical

spectrum, beam quality and temporal features of the laser, is measured and recorded in the experiments.

4. Brightness enhancement by pump ratio optimization

To improve laser brightness, the performance of the NLFA is investigated with different bi-directional pumping ratios. The seed power injected into the amplifier is about 20 W with the measured beam quality of $M^2 \sim 1.25$. The feedback power is measured as about 440 mW. During the laser operation, the feedback power could remain stable, which is critical to laser performance. Figure 3 depicts the output power and the conversion efficiency at pumping ratios of 1:1.9, 1:3.3 and 1:6.4, respectively. In the process of power amplification, the forward pump power is increased firstly, and then the backward pump power is increased until the laser brightness decreases or the beam quality degrades. One can conclude from the variation of different color blocks that more backward pump power could be injected while less forward pumping power is set. In addition, when the forward and backward pumping ratio changes from 1:1.9 to 1:6.4, the final output power improves from 4150 to 5005 W. Defining the optical–optical efficiency as the ratio of output power minus input seed power to the pump power of the amplifier, the value at the maximum laser output is 82.8% with the total pump power of 6020 W.

Figure 4 demonstrates the results of output spectra with different pumping ratios. The maximum signal to noise ratio (SNR) can be over 60 dB in the entire spectral range. The output spectra at different powers with the forward and backward pumping ratio of 1:1.9 are shown in Figure 4(a). Spectral peaks at approximately 1100 nm caused by the FWM effect can be observed once output power exceeded 3 kW. When the output power reached 4150 W, the signal to Raman ratio was about 28.7 dB. Figure 4(b) shows the output spectra at the pumping ratio of 1:3.3. The output power reached 4492 W at a similar SNR level. Furthermore, the output power exceeded 5 kW when the pumping ratio was further decreased to 1:6.4, and no FWM occurred even at the maximum power, as shown in Figure 4(c). These results
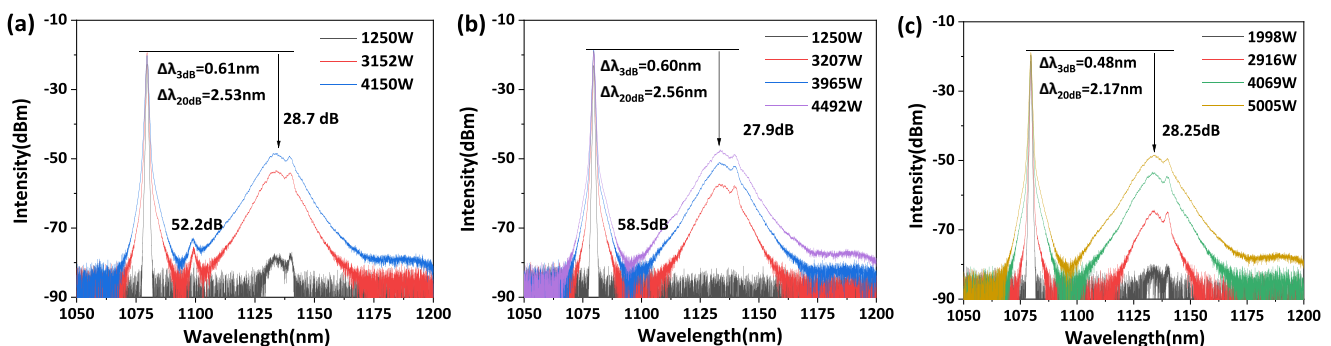

Figure 4. Results of output spectra at different pumping ratios: (a) 1:1.9, (b) 1:3.3 and (c) 1:6.4.
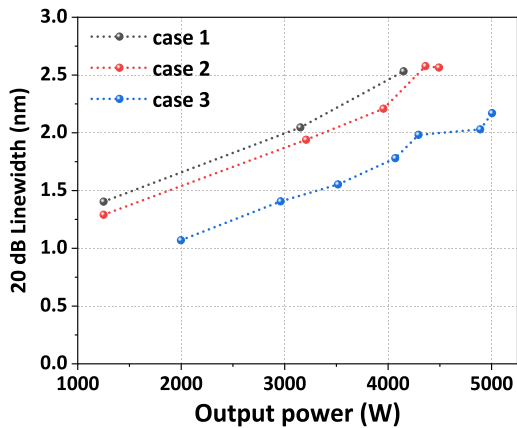
Figure 5. The evolution of 20 dB linewidth versus the output power for different cases.

show that the SRS and FWM effects are mitigated obviously by decreasing the proportion of the forward pump power. In a fiber MOPA amplifier, the forward pumping scheme would result in a higher average signal power along the gain fiber and a longer effective nonlinear length. Therefore, the thresholds of SRS and FWM are reduced with the forward and backward pumping ratio decreasing[21].

Moreover, it is worth noting the variation of signal linewidth versus laser power. With the power increasing, the spectral broadening is the results of SPM and cross-phase modulation (XPM) effects induced by the temporal instability of the laser. Comparing the final linewidth evolution results among the three cases, the 3 and 20 dB signal linewidths are reduced from 0.61 and 2.53 nm of case 1 to 0.48 and 2.1 nm of case 3, respectively. This can also be attributed to a shorter effective length in case 3. Accordingly, the rate of spectral broadening in the backward pumping scheme would be slower compared with the forward pumping scheme as power scaling. With the forward and backward pump powers injected successively, the linewidth increases at different rates separately. After a relatively low forward pump power is injected, there is a narrower signal linewidth before increasing the backward pump power. Then, the signal linewidth grows in the three

cases at a similar trend with the backward pump injecting. Therefore, it is possible to get a narrower linewidth at a higher output power. This process can be depicted clearly according to the evolution of the 20 dB linewidth in the three cases, as shown in Figure 5.

Among the amplification results of the three different pumping ratios, the phenomenon of SRS-induced mode distortion is observed. By calculating spectral integration over the Stokes light, the evolution of the SRS ratio and beam quality versus output power are as depicted in Figure 6. It can be seen the increasing trend between the SRS ratio and M^2 factor is rather similar in cases 1 and 2, which is suggestive of a certain correlation. When the Raman ratio exceeds 2%, the beam quality degrades obviously, from near single mode to approximately 1.7 of the M^2 factor. Research shows this SRS-induced mode distortion is attributed to the core-pumped Raman effect. Energy would transfer irreversibly from the fundamental mode (FM) to high-order modes (HOMs) once the Raman light reaches its threshold, contributing to the degradation of beam quality[32]. However, when the power increased above 4500 W in case 3, the M^2 factor did not increase monotonically with the increase of SRS ratio. This abnormal phenomenon was observed in Ref. [33] and was interpreted as the SRS effect of multimode laser beams. Due to the dynamic change of FM and HOMs at the signal wave-length in core-pumped Raman fiber lasers, the FM of signal light reached the Raman light firstly as power scaling. When the HOMs of signal light reached the Raman threshold, the HOMs would be consumed and weaken the SRS-induced mode distortion. Once the consuming of HOMs outweigh the generating of HOMs, the M^2 factor would decrease for a limited time. One can see that the M^2 factor of 5 kW level NLFA is about 1.35 and the beam quality is almost not deteriorated.

To further identify the correlation between the beam quality and SRS effect, Figure 7 compares the temporal characteristics at the maximum output power with three different pump conditions. It is well known that the sign of TMI is energy transfer at a frequency of the kHz level between the FM and the HOMs[34]. By analyzing the time trace from the photodetector (PD) and their corresponding fast Fourier
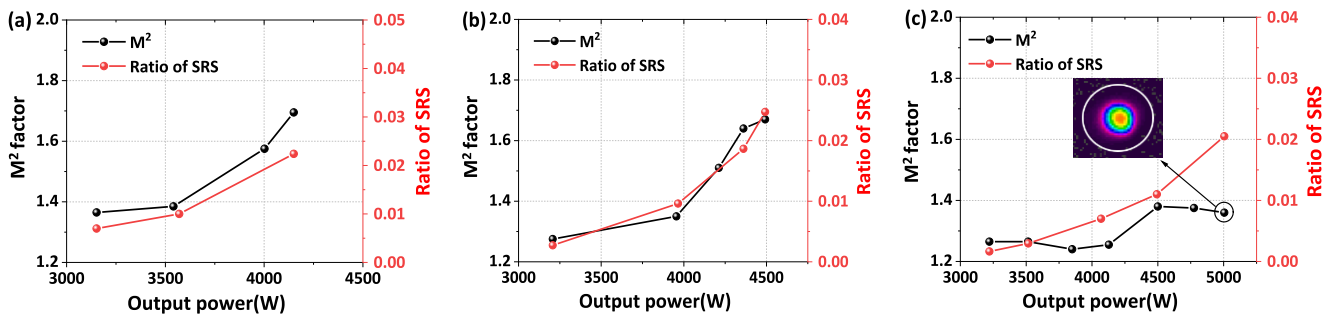

Figure 6. The evolution of ratio of SRS and beam quality versus output power: (a) case 1; (b) case 2; (c) case 3 (inset: beam spot at 5005 W).
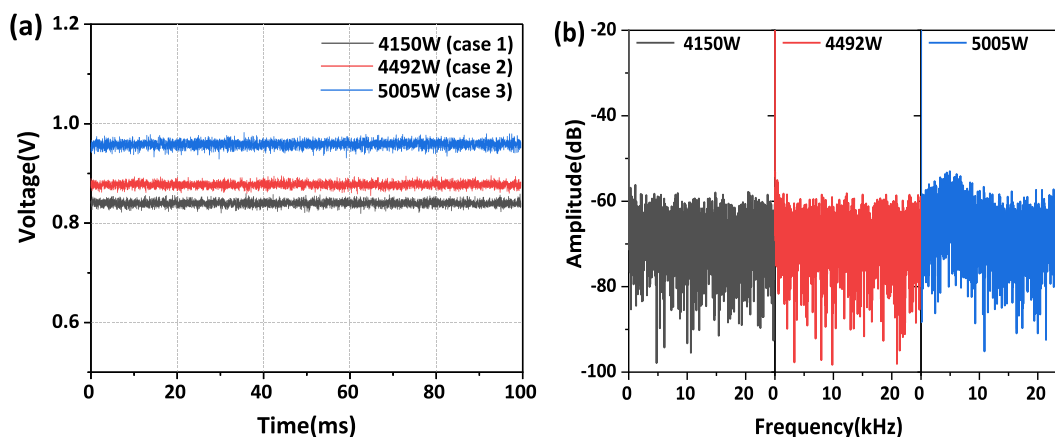
Figure 7. Temporal characteristics at the final output power in the three cases: (a) signals of the PD and (b) results of FFT.

Table 1. The experimental results with different bi-directional pumping ratios.

Case	Output power (W)	Forward/backward pump power (W)	Pumping ratio	3-dB/20-dB linewidth (nm)	SRS ratio	M^2	TMI
1	4150	1748/3248	~1:1.9	0.61/2.53	2.2%	1.7	No
2	4492	1320/4420	~1:3.3	0.60/2.56	2.5%	1.66	No
3	5005	845/5175	~1:6.4	0.48/2.17	2.0%	1.35	Yes

transform (FFT) results, there are no signs of TMI in case 1 or case 2. Thus, it can be inferred that the degradation of beam quality results from the SRS effect rather than TMI. For case 3, it is found that the periodical fluctuations of time traces are not obvious but frequency fluctuations are apparent in the range of 0–5 kHz, indicating that TMI is activated in this fiber amplifier. Based on the results, the TMI threshold can be estimated to be around 5 kW. Considering the capacity of the backward pump combiner, the pump power did not increase continuously after the emergence of TMI. For the phenomenon that the beam quality could be maintained, it can be explained from the increased HOM loss in the gain fiber induced by coiling. The occurrence of TMI causes the increase of content of HOMs in the fiber core. Owing to the bending loss, the coupled HOMs leak into the inner cladding of the fiber and could be dumped in the CLS regions. Therefore, the abnormal phenomenon of the reduced M^2 factor at 5005 W is a result of the comprehensive effects of TMI and the SRS effect in multimode laser beams.

Table 1 summarizes the experimental results of the three different pumping ratios. One can conclude that the various nonlinear effects and SRS-induced mode distortion in the amplifier are suppressed comprehensively by adjusting the bi-directional pumping ratio, accompanied with an improvement of laser power and laser brightness. The laser brightness is 1.9 times that of the original according to the above-mentioned formula. The further brightness enhancement is limited by TMI. Actually, it is also urgent to mitigate the SRS effect because the Raman light to signal ratio is about to reach the degradation threshold of the beam quality.

5. Brightness enhancement by transverse mode instability suppression

To further improve the output power and laser brightness, some designs have to be applied in the NLFA system for mitigating the SRS and TMI effects comprehensively. First of all, a home-made integrated output device including a PSC, CLS and QBH without any melting points is reattached after the gain fiber. The fiber length is decreased from 3 to 1.5 m, which is helpful to weaken the SRS effect while maintaining beam quality. Secondly, the coiling shape of the gain fiber is optimized in the amplifier for raising the TMI threshold, as shown in Figure 8. It has been reported that the fiber coiling or bending diameter is highly dependent on the TMI thresholds in multimode fiber amplifiers[34]. A higher TMI threshold can be obtained by further reducing the bend diameter, but a bend diameter that is too small will induce a high bend loss of FM, which will decrease the efficiency and increase the thermal effects. Considering the above factors, the minimum bending diameter for gain fiber is set to 8 cm. Comparing with the original coiling shape I of 5 kW NLFA, shapes II and III increase the loss of HOMs by introducing more bending parts. The curvature radius of the adjusted parts ranges from 45 to 58 mm.

We experimentally investigated the TMI threshold of the fiber amplifier with different gain fiber coiling shapes. Referring to the pumping ratio of the 5 kW NFLA system, we achieved an output power of 5.5 kW with an M^2 factor of 1.35 by employing coiling shape II for the YDF. The TMI threshold was improved by approximately 500 W and the optical-to-optical efficiency did not decrease, which demonstrates
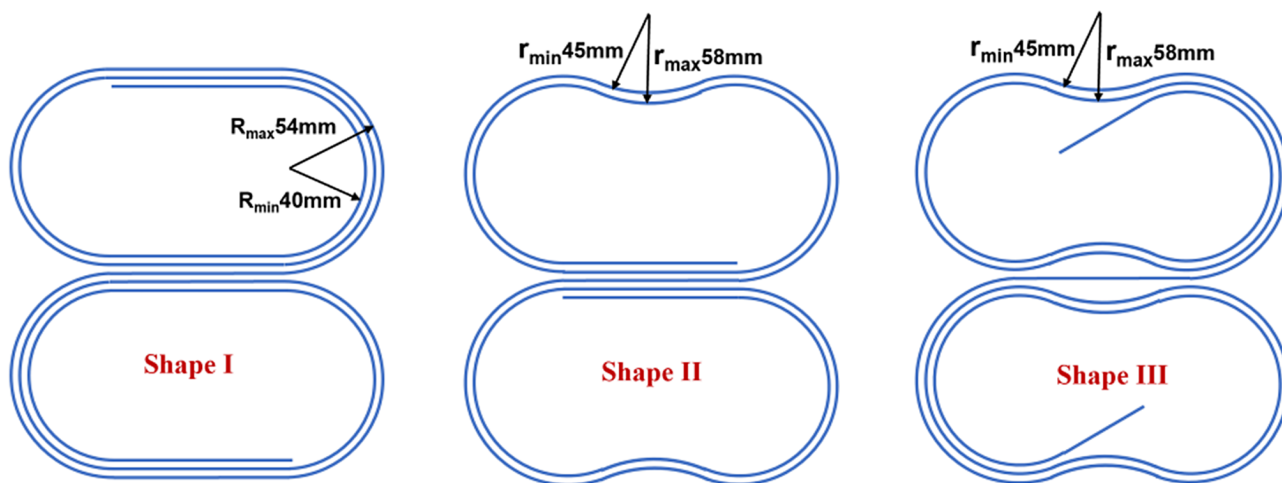
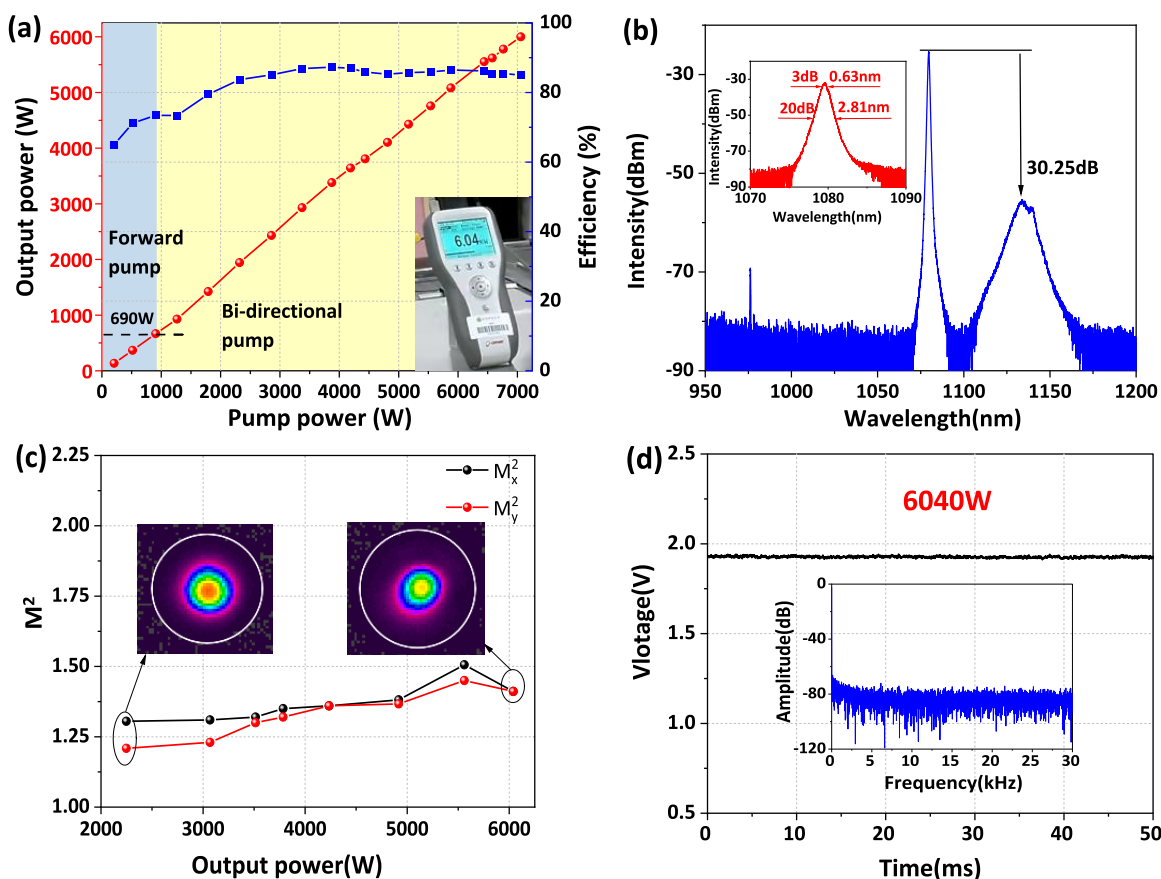**Figure 8.** Diagram of the coiling shape for gain fiber.

Figure 9. (a) The variation curves of the output laser power and the optical-to-optical efficiency with the pump power. (b) The output spectrum at 6 kW. (c) The evolution of beam quality with output power. (d) The signal of the PD at the maximum output power and the FFT result.

that the coiling method of gain fiber has potential to enhance the output brightness. Furthermore, a final 6040 W NLFA system was obtained by using coiling shape III for the YDF. The total pump power was 7058 W with a forward and backward pumping ratio of around 1:6.8. Figure 9(a) shows the evolution of output power and optical-to-optical efficiency with the pump power. The conversion efficiency is 85.0% at the maximum power. As shown in Figure 9(b), the output spectrum at 6 kW has no sign of FWM and the SNR is 30.25 dB. By integral operation of the spectrum, the Stokes components (1100–1175 nm) take up 1.4% of the total power. The 3 and 20 dB linewidths are 0.63 and 2.81 nm, respectively. Figure 9(c) shows the evolution of beam quality with output power. Thanks to the suppression
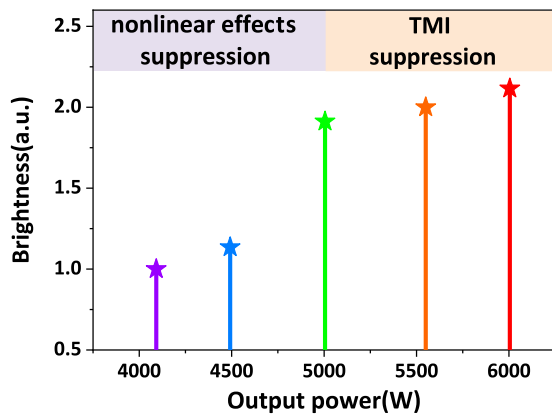
Figure 10. The results of laser brightness enhancement.

of the TMI and SRS effects, the output laser maintained nearly single-mode operation during the power scaling and the beam quality M^2 was approximately 1.41 at 6 kW. The temporal signal detected by the PD and its corresponding FFT spectrum are shown in Figure 9(d). The slight frequency fluctuation on the FFT spectrum indicates that the NLFA worked around the TMI threshold. The maximum backward power monitored from the BPFC was about 1.6 W. The laser system withstood 10 minutes of testing and performed stably with power fluctuation of less than 0.3%.

Figure 10 lists the evolution of laser brightness during the optimization process. By adjusting the bi-directional pumping ratio, various nonlinear effects are mitigated. The laser output power and brightness increase obviously with an enhancement of 90%. With the method of novel coiling for gain fiber, the TMI threshold improves by approximately 1000 W and laser brightness is further enhanced by a factor of 2.1. Finally, a 6 kW NLFA is achieved with the highest brightness based on the simple MOPA structure.

6. Conclusion

In conclusion, a near single-mode 6 kW narrow-linewidth fiber laser based on a simple MOPA structure has been demonstrated for the first time. The methods of optimizing the temporal characteristics of the FBG-based seed have been adopted by utilizing a novel cavity structure. After decreasing the pumping ratios of the amplifier stage, the SRS, FWM and spectral broadening effects are suppressed simultaneously, so that the output power and laser brightness improve together. By adopting a new coiling type for gain fiber of the amplifier further, the TMI threshold of the system is further improved. The laser brightness is further enhanced by a factor of over 2. Finally, with total pump power of 7058 W (pumping ratio of 1:6.8), a 6-kW fiber laser is achieved with optical-to-optical efficiency of 85.0%. At the maximum output power, the SNR is 30.25 dB and the beam quality M^2 factor is approximately 1.4. The 3 and

20 dB linewidths are 0.63 and 2.81 nm, respectively. Overall, this work could provide a good reference for the power scaling of narrow-linewidth fiber lasers based on the simple MOPA structure. The modified seed structure with optimized temporal characteristics and the novel fiber coiling method are universal for SRS and TMI suppression respectively in traditional fiber amplifiers.

Acknowledgement

References

1. C. Jauregui, J. Limpert, and A. Tünnermann, Nat. Photonics **7**, 861 (2013).
2. D. J. Richardson, J. Nilsson, and W. A. Clarkson, J. Opt. Soc. Am. B **11**, 27 (2010).
3. M. N. Zervas, and C. A. Codemard, IEEE J. Select. Top. Quantum Electron. **5**, 20 (2014).
4. W. Liu, P. Ma, H. Lv, J. Xu, P. Zhou, and Z. Jiang, Opt. Express **24**, 26715 (2016).
5. J. W. Dawson, M. J. Messerly, R. J. Beach, M. Y. Shverdin, E. A. Stappaerts, A. K. Sridharan, P. H. Pax, J. E. Heebner, C. W. Siders, and C. P. J. Barty, Opt. Express **17**, 16 (2008).
6. T. Eidam, C. Wirth, C. Jauregui, F. Stutzki, F. Jansen, H. J. Otto, O. Schmidt, T. Schreiber, J. Limpert, and A. Tunnermann, Opt. Express **14**, 19 (2011).
7. R. Tao, X. Wang, and P. Zhou, IEEE J. Select. Top. Quantum Electron. **24**, 0903319 (2018).
8. S. J. McNaught, P. A. Thielen, L. N. Adams, J. G. Ho, A. M. Johnson, J. P. Machan, J. E. Rothenberg, C.-C. Shih, D. M. Shimabukuro, M. P. Wacks, M. E. Weber, and G. D. Goodno, IEEE J. Select. Top. Quantum Electron. **20**, 174 (2014).
9. Z. Liu, P. Ma, R. Su, R. Tao, Y. Ma, X. Wang, and P. Zhou, J. Opt. Soc. Am. B **34**, A7 (2017).
10. Y. Zheng, Y. Yang, J. Wang, M. Hu, G. Liu, X. Zhao, X. Chen, K. Liu, C. Zhao, B. He, and J. Zhou, Opt. Express **24**, 12063 (2016).
11. T. Loftus, A. Thomas, P. Hoffman, M. Norsen, R. Royse, A. Liu, and E. Honea, IEEE J. Select. Top. Quantum Electron. **13**, 487 (2007).
12. A. Flores, C. Robin, A. Lanari, and I. Dajani, Opt. Express **22**, 17735 (2014).
13. I. Dajani, A. Flores, R. Holten, B. Anderson, B. Pulford, and T. Ehrenreich, Proc. of SPIE **9728**, 972801 (2016).
14. M. Liu, Y. Yang, H. Shen, J. Zhang, X. Zou, H. Wang, L. Yuan, Y. You, G. Bai, B. He, and J. Zhou, Sci. Rep. **10**, 629 (2020).
15. C. Yu, O. Shatrovoy, T. Fan, and T. Taunay, Opt. Lett. **41**, 5202 (2016).
16. A. Harish and J. Nilsson, Opt. Express **23**, 6988 (2015).
17. Z. Huang, Q. Shu, R. Tao, Q. Chu, Y. Luo, D. Yan, X. Feng, Y. Liu, W. Wu, H. Zhang, H. Lin, J. Wang, and F. Jing, Photon. Technol. Lett. **33**, 1181 (2021).
18. G. Wang, J. Song, Y. Chen, S. Ren, P. Ma, W. Liu, T. Yao, and P. Zhou, High Pow Laser Sci. Eng. **10**, e22 (2022).
19. P. Ma, T. Yao, Y. Chen, G. Wang, S. Ren, W. Li, W. Liu, Z. Pan, L. Huang, Z. Chen, P. Zhou, and J. Chen, Proc. SPIE **12310**, 123100E (2022).
20. Y. Huang, Q. Xiao, D. Li, J. Xin, Z. Wang, J. Tian, Y. Wu, M. Gong, L. Zhu, and P. Yan, Opt. Laser Technol. **133**, 106538 (2021).

21. S. Du, G. Fu, T. Qi, C. Li, Z. Huang, D. Li, P. Yan, M. Gong, and Q. Xiao, Opt. Fiber Technol. **73**, 103011 (2022).
22. X. Tian, B. Rao, X. Xi, M. Wang, C. Wang, and Z. Wang, Opt. Express **31**, 12016 (2023).
23. S. Liao, T. Luo, R. Xiao, C. Shu, J. Cheng, Z. Zhang, Y. Xing, H. Li, N. Dai, and J. Li, Opt. Lett. **48**, 6533 (2023).
24. A. E. Bednyakova, O. A. Gorbunov, M. O. Politko, S. I. Kablukov, S. V. Smirnov, D. V. Churkin, M. P. Fedoruk, and S. A. Babin, Opt. Express **21**, 8177 (2013).
25. W. Liu, P. Ma, H. Lv, J. Xu, P. Zhou, and Z. Jiang, Opt. Express **24**, 8708 (2016).
26. S. Zhang, W. Zhang, M. Jiang, W. Liu, P. Ma, C. Li, R. Su, P. Zhou, and Z. Jiang, Appl. Opt. **60**, 5984 (2021).
27. W. Liu, P. Ma, and P. Zhou, J. Opt. Soc. Am. B **38**, 3663 (2021).
28. T. Li, W. Ke, Y. Ma, Y. Sun, and Q. Gao, J. Opt. Soc. Am. B **36**, 1457 (2019).
29. X. Tian, B. Rao, M. Wang, X. Xi, C. Wang, W. Liu, P. Ma, Z. Chen, H. Xiao, H. Fang, and Z. Wang, IEEE Photon. Technol. Lett. **35**, 1175 (2023).
30. V. Bock, A. Liem, T. Schreiber, R. Eberhardt, A. Tünnermann, in *Fiber Lasers XV: Technology and Systems* (SPIE, San Francisco, United States, 2018), p. 50.
31. H. Xu, M. Jiang, P. Zhou, G. Zhao, and X. Gu, Appl. Opt. **56**, 9079 (2017).
32. C. Zhang, R. Tao, M. Li, X. Feng, R. Liao, Q. Chu, L. Xie, H. Li, B. Shen, L. Xu, and J. Wang, J. Lightwave Technol. **41**, 671 (2023).
33. C. Zhang, L. Xie, H. Li, B. Shen, X. Feng, M. Li, R. Tao, and J. Wang, IEEE Photonics J. **14**, 3016605 (2022).
34. F. Zhang, H. Xu, Y. Xing, S. Hou, Y. Chen, J. Li, N. Dai, H. Li, Y. Wang, and L. Liao, Laser Phys. Lett. **16**, 035104 (2019).